

Sonochemical Synthesis of Photoluminescent Nanoscale Eu(III)-Containing Metal-Organic Frameworks

Cheng-an TAO¹, Zhihong HU¹, Lingqiang MENG², Fang WANG¹, Jianfang WANG^{1*}

¹ College of Science, National University of Defense Technology, Changsha 410073, Hunan, P. R. China

² Yanching Institute of Technology, Sanhe, 065201, Hebei, P. R. China

crossref <http://dx.doi.org/10.5755/j01.ms.21.4.9695>

Received 28 January 2015; accepted 03 October 2015

Nanoscale lanthanide-containing metal-organic frameworks (MOFs) have more and more interest due to their great properties and potential applications, but how to construct them easily is still challenging. Here, we present a facile and rapid synthesis of Eu(III)-containing Nanoscale MOF (denoted as NMOF) under ultrasonic irradiation. The effect of the ratio and the addition order of metal ions and linkers on the morphology and size of MOFs was investigated. It is found that both of the ratio and the addition order can affect the morphology and size of 1,4-benzenedicarboxylic acid(H₂BDC)-based MOFs, but they show no evident influence on that of H₂aBDC-based MOFs. The former exhibit typical emission bands of Eu(III) ions, while the latter only show the photoluminescent properties of ligands.

Keywords: sonochemical, metal-organic frameworks, lanthanide, nanoscale, luminescent.

1. INTRODUCTION

Metal organic frameworks (MOFs), also called porous coordination polymers (PCPs) are hybrid inorganic-organic crystalline porous materials made from an assembly of metal ions with organic linkers [1–3]. Their unique properties, such as well-defined and high porosity, large internal surface areas, thermal stability and tunable chemical functionality etc., make them extremely attractive for applications in gas storage [4], separation [5, 6], and catalysis [7–9].

Among them, lanthanide-containing MOFs (LnMOF) have attracted great interest because they usually exhibit excellent luminescent performance-emitting intensely over narrow wavelength ranges, and are promising candidates for the design of luminescent materials and devices [10–13]. Bulky LnMOFs have been extensively investigated. To further explore the applications of LnMOFs, the bulky LnMOFs need to be scaled down to the nanoregime to form nanoscale MOFs (NMOFs), which perform different functionality from the bulky one because of the straightforward transportation property and/or interaction within the nanoscale materials [14]. For example, NMOFs can be potentially used in magnetic resonance imaging, biolabeling, biosensing, drug delivery and so on [15, 16]. More and more investigations have been focused on the design and preparation of NMOFs, however, the study on functional nanoscale LnMOFs is still at the very early stage [15, 17–20]. Especially, the construction of NMOFs efficiently is still a very challenging issue.

To date several methods have been developed for fabricating NMOFs, such as solvent diffusion approach [21], reverse microemulsion [20], and microwave-assisted synthesis [22]. Solvent diffusion approach usually costs

long reaction times and a large amount of solvent. Reverse microemulsion method also requires a large amount of solvent as well as surfactants. Microwave-assisted synthesis has been demonstrated to be very efficient and eco-friendly, but it is difficult to tune the dimensionality of the nanocrystals of MOFs. Recently, ultrasonic synthesis has been proposed as a simple, efficient, low cost, and eco-friendly approach to NMOF [14, 23–29]. Many MOFs, such as Zn₃(BTC)₂·12H₂O [23], MIL-53(Fe) [24], HKUST-1 [25], MOF-5 [26], Mg-MOF-74 [27], PCN-6/PCN-6' [28], IRMOF-9/IRMOF-10 [28], ZIF-8 [29], {[Zn(ip)(bpy)]_n} [14], have been prepared via sonochemical approach, but nanoscale LnMOFs made via this approach have been rarely explored.

In this context, we present a facile and rapid synthesis of Eu(III)-containing NMOF under ultrasonic irradiation. The effect of the ratio of metal ions and linkers on the morphology and size of LnMOFs as well as the effect of the addition order was investigated. Two kinds of linkers, 1,4-benzenedicarboxylic acid(H₂BDC) and 2-amino-1,4-benzenedicarboxylic acid(H₂aBDC) were used respectively. The resultant LnMOFs were observed by scanning electron microscope (SEM) and transmission electron microscope (TEM). The Photoluminescent properties of them were also characterized.

2. EXPERIMENTAL METHODS

2.1. Materials

H₂BDC (99 %) and H₂aBDC (99 %) were purchased from Alfa Aesar. Europium(III) acetate hydrate (Eu(OAc)₃·6H₂O), *N,N*-dimethylformamide (99.8 %, DMF) and other chemicals were purchased from local chemicals. All chemicals were used as received.

2.2. Ultrasonic Synthesis of LnMOFs

Ultrasonic syntheses of H₂BDC-based LnMOFs were carried out under ultrasonic irradiation at a frequency of

* Corresponding author. Tel.: +86-731-84574784; fax: +86-731-84574250. E-mail address: Wangjianfang@nudt.edu.cn (J. WANG)

40 KHz (KQ3200DE, Kunshan Ultrasonics) at ambient temperature and atmospheric pressure for 10 min, and the ultrasonic output was kept to be 150 W in all experiments. Two series of experiments were performed, one series are as follows: an DMF solution (8 mL) of $\text{Eu}(\text{OAc})_3 \cdot 6\text{H}_2\text{O}$ (5 mM) was added into a test tube (20 mL), and the test tube was fixed in the bath of the ultrasonic generator. Under ultrasonic irradiation, 2 mL of DMF solution of H_2BDC with different concentrations (100, 75, 50, 25, 10 mM) was added into $\text{Eu}(\text{OAc})_3 \cdot 6\text{H}_2\text{O}$ solution. After the ultrasonic irradiation for 10 min, the resulting products were filtered. The products were isolated by filtering the precipitation from reaction mixture, and the precipitation washed with DMF, ethanol and acetone and then dried in vacuum. The products are denoted as A1, A2, A3, A4 and A5, respectively. In the other series of experiments, the order of addition of two solutions is inverted. The products are denoted as B1, B2, B3, B4 and B5, respectively.

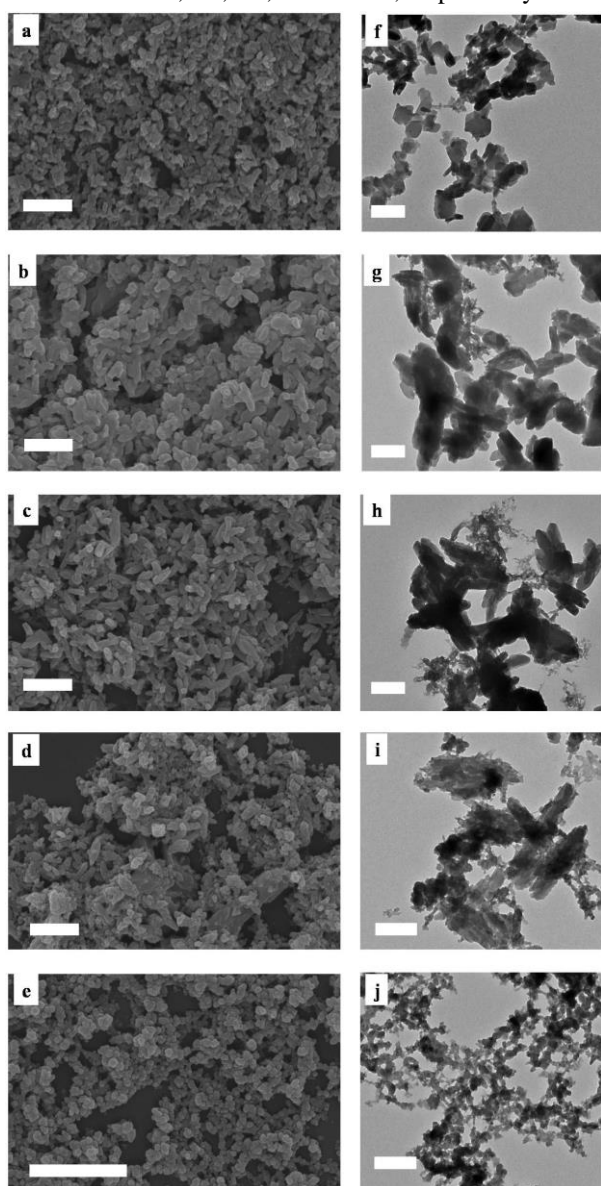


Fig. 1. SEM images: a – e, 1bar=1 μm ; TEM images: f – j, 1bar = 200 nm; a, f – A1; b, g – A2; c, h – A3; d, i – A4; e, j – A5

Ultrasonic syntheses of H_2aBDC -based LnMOFs were carried out in substantially identical condition, only

H_2BDC solution was replaced by H_2aBDC solution. And resultant products are denoted as C1 to C5 and D1 to D5, respectively.

2.3 Characterization

Morphological investigations were carried out using a LEO-1503 field-emission SEM, after sputtering the samples with a thin layer of gold. The TEM images were obtained with Hitachi H-7650B, operating at 80 kV. The samples were prepared by placing a droplet of a suspension onto a carbon-coated Cu grid. Photoluminescence spectra were taken on a Perkin Elmer LS55 fluorescence spectrometer at room temperature.

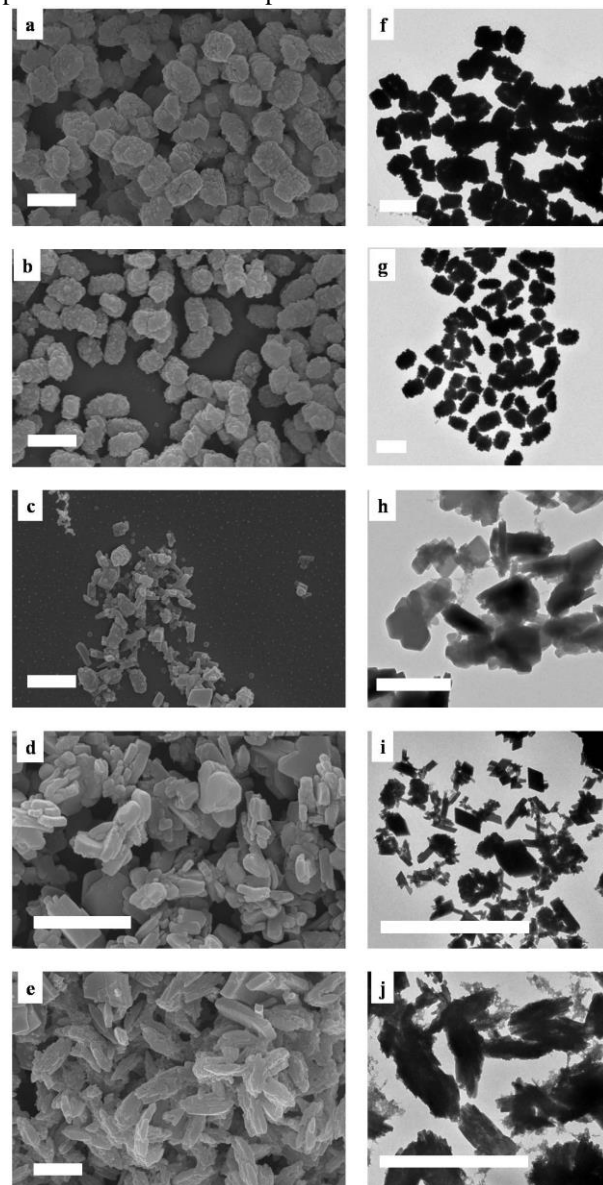


Fig. 2. SEM images: a – e; TEM images: f – j; a, f – B1; b, g – B2; c, h – B3; d, i – B4; e, j – B5; 1 bar = 1 μm

3. RESULTS AND DISCUSSION

3.1. Characterization of LnMOFs

A series products were prepared by adding H_2BDC solution into Eu solution under ultrasonic irradiation. The SEM and TEM images of A1 to A5 were shown in Fig. 1. In the present of high concentration of linkers, the resultant

products, A1 are randomly nanoparticles with sizes of about 130 nm (Fig. 1 a and f). With the decreasing concentration of linkers, both the shape and size of MOFs are drastically changed. Decrease of the concentration of linkers results in fairly uniform rod-like nanocrystals with a length and width of 650 nm and 100 nm, respectively (Fig. 1 c and h). Further decrease the linker concentration, the size of nanoparticles decreased again, only about 50 ± 25 nm, and showed sphere-like morphology (Fig. 1 e and j). Nanoscale LnMOF was successfully synthesized in the sonochemical condition, and the shapes and sizes can be tuned by the ratio of linker and metal ions. For comparison, the order of addition of metal ion and linker solutions is inverted to see whether the order effects on the morphology of the MOFs. SEM and TEM images of resultant LnMOFs were shown in Fig. 2. In the present of high concentration of linkers, nanocrystals of about 30–40 nm formed first and then they aggregated to be larger spheroidicity particles with the length of 800 nm and width of 600 nm (Fig. 2 a and f). In the present of lower concentration, the nanoplates, 100–500 nm in length and 80–120 nm in thickness were obtained (Fig. 2 d and i). Further decrease the concentration of linkers, the obtained nanoplates turned imperfect, which are aggregations of nanorods. The results suggest that the order of addition of the two solutions is important, which determined MOFs how to nucleate in the initial step.

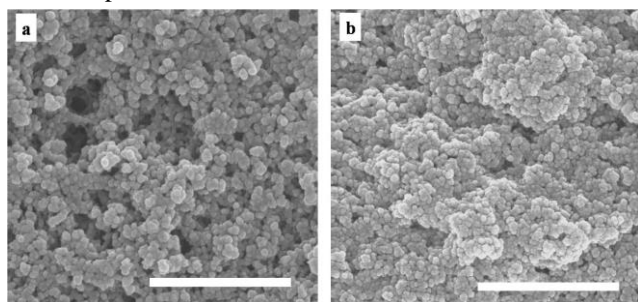


Fig. 3. SEM images: a – C1; b – D5. 1 bar = 1 μ m

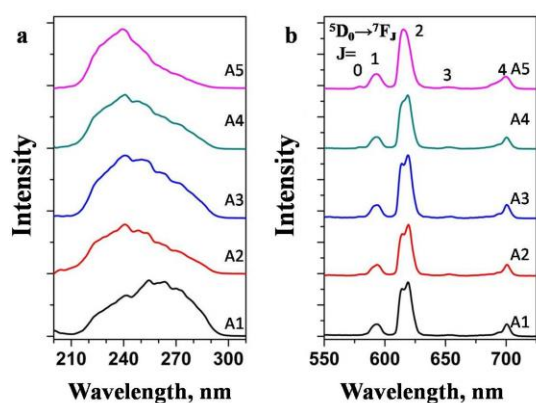


Fig. 4. Excitation (a) and emission (b) spectra of A1 to A5 dispersed in EtOH (excited and monitored at 241 nm and 619 nm, respectively)

Moreover, H₂aBDC was used to replace H₂BDC to synthesize LnMOF under ultrasonic irradiation. It's found that the concentrations of linker has merely influence on the morphology and sizes of obtained nanoparticles,

20–30 nm (Fig. 3 a). The order of addition of the metal and linker solutions was also investigated, the similar sphere-like nanoparticles were obtained, which has no obvious relationship with the addition order (Fig. 3 b).

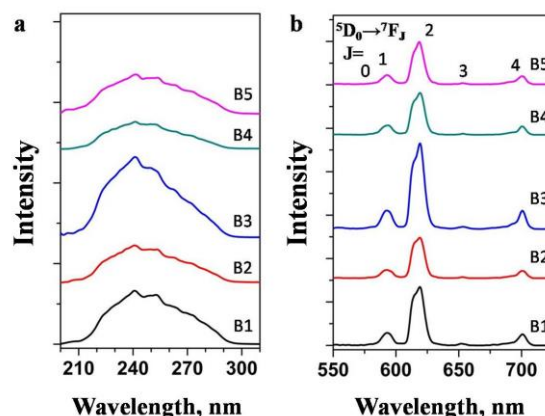


Fig. 5. Excitation (a) and emission (b) spectra of B1 to B5 (excited and monitored at 241 nm and 619 nm, respectively)

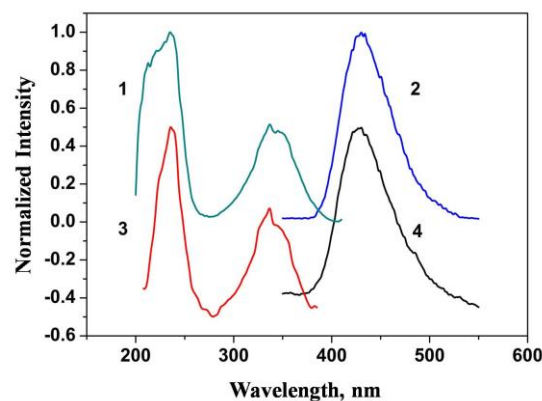


Fig. 6. Excitation (1, 3) and emission (2, 4) spectra of Linker H₂aBDC (1, 2) and LnMOF, C1 (3, 4) (excited and monitored at 241 nm and 430 nm, respectively)

3.2. Photoluminescent properties

Photoluminescence is one important performance of Eu-containing MOFs. Photoluminescent spectra of synthesized LnMOFs were recorded at room temperature with steady-state luminescence spectrometer. Fig. 4 shows the excitation and emission spectra of A1 to A5 (excited and monitored at 241 nm and 619 nm, respectively). The excitation spectra of A1 – A5 products are very similar, and are largely dominated by the ligand bands, pointing to a good antenna effect [30]. The emission spectra exhibit typical emission bands of Eu(III) ions upon excitation at 241 nm. The emission bands arise from $^5D_0 \rightarrow ^7F_j$ ($j = 0, 1, 2, 3$ and 4) transitions of Eu(III) ions [31, 32]. Limitations in the resolution of the spectrometer used prevented us from observing further splitting of the peaks. The $^5D_0 \rightarrow ^7F_0$ and $^5D_0 \rightarrow ^7F_3$ transitions are too weak to be observed. It is well-known that the strong emission at 619 nm is corresponding to $^5D_0 \rightarrow ^7F_2$ transition induced by the electric dipole moment, which is hypersensitive to the coordination environment of the Eu(III) ion [20]. The emission at 591 nm is attributed to the magnetic dipole

induced $^5D_0 \rightarrow ^7F_1$ transition, which is fairly insensitive to the coordination environment of the Eu(III) ion. The intensity ratio of $^5D_0 \rightarrow ^7F_2 / ^5D_0 \rightarrow ^7F_1$ is approximately 5.0, which indicates that the Eu(III) ion is not located at the inversion center and that the symmetry of the Eu(III) ion site is low [33–35]; this is in agreement with the previous reports [36].

Very similar results were observed for B series products, as shown in Fig. 5. While the photoluminescent spectra of Eu-aBDC MOFs are very different from that of A and B series. Fig. 6 shows typical excitation and emission spectra of C1 and the linker H₂aBDC. The excitation spectrum of B1 is largely dominated by the linker bands. And the emission spectra of them are also very similar. There are no obvious typical emission bands of Eu(III) ion. This finding shows that the linker H₂aBDC is not a good antenna for Eu(III) ion, and the H₂aBDC-based LnMOFs only exhibit the photoluminescent properties of ligand.

4. CONCLUSIONS

Nanoscale Eu(III)-containing LnMOFs were successfully synthesized by facile and rapid sonochemical method. The effect of the ratio of metal ions and linkers on the morphology and size of H₂aBDC-based LnMOFs is very evident, and the addition order of metal ion and linker solutions also affects the morphology and size. What's different that neither the ratio of metal ions and linkers nor the ratio of two solutions obviously affects the morphology and size of H₂aBDC-based LnMOFs. H₂aBDC-based LnMOFs exhibit typical emission bands of Eu(III) ions, while the H₂aBDC-based LnMOFs only exhibit the photoluminescent properties of ligand itself. The obtained nanoscale Eu(III)-containing LnMOFs can be used in fluorescence materials, sensing, biolabeling and other photoluminescence related fields.

Acknowledgments

We acknowledge the financial support of National Natural Science Foundation of China (21203247) and Research Project of National University of Defense Technology (JC12-02-12).

REFERENCES

1. Li, H., Eddaoudi, M., O'Keeffe, M., Yaghi, O. M. Design and Synthesis of an Exceptionally Stable and Highly Porous Metal-Organic Framework *Nature* 402 (6759) 1999: pp. 276–279.
2. Férey, G. Hybrid Porous Solids: Past, Present, Future *Chemical Society Review* 37 (1) 2008: pp. 191–214. <http://dx.doi.org/10.1039/B618320B>
3. Zhou, H. C., Long, J. R., Yaghi, O. M. Introduction to Metal-Organic Frameworks *Chemical Review* 112 (2) 2012: pp. 673–674. <http://dx.doi.org/10.1021/cr300014x>
4. Murray, L. J., Dincă, M., Long, J. R. Hydrogen Storage in Metal-Organic Frameworks *Chemical Society Review* 38 (Suppl) 2009: pp. 1294–1314. <http://dx.doi.org/10.1039/b802256a>
5. Li, J.R., Kuppler, R.J., Zhou, H.C. Metal-Organic Frameworks for Separations *Chemical Review* 112 (2) 2012: pp. 869–932.
6. Li, J.R., Kuppler, R.J., Zhou, H.C. Selective Gas Adsorption and Separation in Metal-Organic Frameworks *Chemical Society Review* 38 (5) 2009: pp. 1477–1504. <http://dx.doi.org/10.1039/b802426j>
7. Ma, L., Abney, C., Lin, W. Enantioselective Catalysis with Homochiral Metal-Organic Frameworks *Chemical Society Review* 38 (5) 2009: pp. 1248–1256. <http://dx.doi.org/10.1039/b807083k>
8. Lee, J., Farha, O.K., Roberts, J., Scheidt, K.A., Nguyen, S.T., Hupp, J.T. Metal-Organic Framework Materials as Catalysts *Chemical Society Review* 38 (5) 2009: pp. 1450–1459.
9. Corma, A., García, H., Llabrés I Xamena, F. X. Engineering Metal Organic Frameworks for Heterogeneous Catalysis *Chemical Review* 110 (8) 2010: pp. 4606–4655.
10. Evans, R.C., Douglas, P., Winscom, C.J. Coordination Complexes Exhibiting Room-Temperature Phosphorescence: Evaluation of their Suitability as Triplet Emitters in Organic Light Emitting Diodes *Coordination Chemical Review* 250 (15–16) 2006: pp. 2093–2126.
11. Black, C.A., Costa, J.S., Fu, W.T., Massera, C., Roubeau, O., Teat, S.J., Aromí, G., Gamez, P., Reedijk, J. 3-D Lanthanide Metal-Organic Frameworks: Structure, Photoluminescence, and Magnetism *Inorganic Chemistry* 48 (3) 2009: pp. 1062–1068.
12. Daignebonne, C., Kerbellec, N., Guillou, O., Bünzli, J.C., Gummy, F., Catala, L., Mallah, T., Audebrand, N., Gérald, Y., Bernot, K., Calvez, G. Structural and Luminescent Properties of Micro- and Nanosized Particles of Lanthanide Terephthalate Coordination Polymers *Inorganic Chemistry* 47 (9) 2008: pp. 3700–3708.
13. Qu, Y., Ke, Y., Lu, S., Fan, R., Pan, G., Li, J. Hydrothermal Synthesis, Structures and Spectroscopy of 2D Lanthanide Coordination Polymers Built from Helical Chains: [Ln₂(BDC)₃(H₂O)₂]_n (Ln=Sm, 1, Ln=Eu, 2; BDC=1,3-benzenedicarboxylate) *Journal of Molecular Structure* 734 (1–3) 2005: pp. 7–13.
14. Tanaka, D., Henke, A., Albrecht, K., Moeller, M., Nakagawa, K., Kitagawa, S., Groll, J. Rapid Preparation of Flexible Porous Coordination Polymer Nanocrystals with Accelerated Guest Adsorption Kinetics *Nature Chemistry* 2 (5) 2010: pp. 410–416.
15. Lin, W., Rieter, W.J., Taylor, K.M.L. Modular Synthesis of Functional Nanoscale Coordination Polymers *Angewandte Chemie International Edition* 48 (4) 2009: pp. 650–658.
16. Spokoyny, A.M., Kim, D., Sumrein, A., Mirkin, C.A. Infinite Coordination Polymer Nano- and Microparticle Structures *Chemical Society Review* 38 (5) 2009: pp. 1218–1227.
17. Kerbellec, N., Catala, L., Daignebonne, C., Gloter, A., Stephan, O., Bünzli, J. C., Guillou, O., Mallah, T. Luminescent Coordination Nanoparticles *New Journal of Chemistry* 32 (4) 2008: pp. 584–587. <http://dx.doi.org/10.1039/b719146d>
18. Sun, X., Dong, S., Wang, E. Coordination-induced Formation of Submicrometer-scale, Monodisperse, Spherical Colloids of Organic-inorganic Hybrid Materials at Room Temperature *Journal of the American Chemical Society* 127 (38) 2005: pp. 13102–13103.

19. **Imaz, I., Hernando, J., Ruiz-Molina, D., Maspoch, D.** Metal-organic Spheres as Functional Systems for Guest Encapsulation *Angewandte Chemie International Edition* 48 (13) 2009: pp. 2325–2329.
20. **Rieter, W.J., Taylor, K.M.L., An, H., Lin, W., Lin, W.** Nanoscale Metal-organic Frameworks as Potential Multimodal Contrast Enhancing Agents *Journal of the American Chemical Society* 128 (10) 2006: pp. 9024–9025.
21. **Jeon, Y.M., Heo, J., Mirkin, C.A.** Dynamic Interconversion of Amorphous Microparticles and Crystalline Rods in Salen-Based Homochiral Infinite Coordination Polymers *Journal of the American Chemical Society* 129 (24) 2007: pp. 7480–7481.
<http://dx.doi.org/10.1021/ja071046w>
22. **Ni, Z., Masel, R.I.** Rapid Production of Metal-Organic Frameworks via Microwave-Assisted Solvothermal Synthesis *Journal of the American Chemical Society* 128 (38) 2006: pp. 12394–12395.
<http://dx.doi.org/10.1021/ja0635231>
23. **Qiu, L. G., Li, Z. Q., Wu, Y., Xu, T., Jiang, X.** Facile Synthesis of Nanocrystals of a Microporous Metal-organic Framework by an Ultrasonic Method and Selective Sensing of Organoamines *Chemical Communications* 44 (31) 2008: pp. 3642–3644.
24. **Gordon, J., Kazemian, H., Rohani, S.** Rapid and Efficient Crystallization of MIL-53(Fe) by Ultrasound and Microwave Irradiation *Microporous and Mesoporous Materials* 162 (6) 2012: pp. 36–43.
25. **Li, Z.Q., Qiu, L.G., Xu, T., Wu, Y., Wang, W., Wu, Z.Y., Jiang, X.** Ultrasonic Synthesis of the Microporous Metal-organic Framework $\text{Cu}_3(\text{BTC})_2$ at Ambient Temperature and Pressure: An Efficient and Environmentally Friendly Method *Material Letters* 63 (1) 2009: pp. 78–80.
26. **Son, W.J., Kim, J., Kim, J., Ahn, W.S.** Sonochemical Synthesis of MOF-5 *Chemical Communications* 44 (47) 2008: pp. 6336–6338.
<http://dx.doi.org/10.1039/b814740j>
27. **Yang, D. A., Cho, H. Y., Kim, J., Yang, S. T., Ahn, W. S.** CO_2 Capture and Conversion using Mg-MOF-74 Prepared by a Sonochemical Method *Energy Environmental Science* 5 (4) 2012: pp. 6465–6473.
28. **Kim, J., Yang, S. T., Choi, S. B., Sim, J., Kim, J., Ahn, W. S.** Control of catenation in CuTATB-n Metal-Organic Frameworks by Sonochemical Synthesis and its Effect on CO_2 Adsorption *Journal of Materials Chemistry* 21 (9) 2011: pp. 3070–3076.
<http://dx.doi.org/10.1039/c0jm03318a>
29. **Cho, H.Y., Kim, J., Kim, S.N., Ahn, W.S.** High yield 1-L Scale Synthesis of ZIF-8 via a Sonochemical Route *Microporous and Mesoporous Materials* 169 (4) 2013: pp. 180–184.
30. **Guo, X., Zhu, G., Sun, F., Li, Z., Zhao, X., Li, X., Wang, H., Qiu, S.** Synthesis, Structure, and Luminescent Properties of Microporous Lanthanide Metal-Organic Frameworks with Inorganic Rod-Shaped Building Units *Inorganic Chemistry* 45 (6) 2006: pp. 2581–2587.
<http://dx.doi.org/10.1021/ic0518881>
31. **de Bettencourt-Dias, A.** Isophthalato-based 2D Coordination Polymers of Eu(III), Gd(III), and Tb(III): Enhancement of the Terbium-centered Luminescence Through Thiophene Derivatization *Inorganic Chemistry* 44 (8) 2005: pp. 2734–2741.
32. **Law, G.L., Wong, K.L., Zhou, X., Wong, W.T., Tanner, P.A.** Crystal Structure and Luminescence of Lanthanide Monodentate Complexes $[\text{Ln}(\text{C}_4\text{N}_4\text{H}_6\text{O})_2(\text{H}_2\text{O})_6]\text{Cl}_3$ and $[\text{Ln}(\text{C}_4\text{N}_4\text{H}_6\text{O})_2(\text{H}_2\text{O})_3(\text{NO}_3)_3]$ (Ln = Tb or Eu) *Inorganic Chemistry* 44 (12) 2005: pp. 4142–4144.
<http://dx.doi.org/10.1021/ic050115+>
33. **Han, Y., Li, X., Li, L., Ma, C., Shen, Z., Song, Y., You, X.** Structures and Properties of Porous Coordination Polymers based on Lanthanide Carboxylate Building Units *Inorganic Chemistry* 49 (23) 2010: pp. 10781–10787.
34. **Yang, X.P., Jones, R.A., Rivers, J.H., Lai, R.P.** Syntheses, Structures and Luminescent Properties of New Lanthanide-based Coordination Polymers based on 1,4-Benzenedicarboxylate (bdc) *Dalton Transactions* 26 (35) 2007: pp. 3936–3942.
<http://dx.doi.org/10.1039/b706823a>
35. **Liu, C.B., Sun, C.Y., Jin, L.P., Lu, S.Z.** Supramolecular Architecture of New Lanthanide Coordination Polymers of 2-Aminoterephthalic Acid and 1,10-Phenanthroline *New Journal of Chemistry* 28 (8) 2004: pp. 1019–1026.
<http://dx.doi.org/10.1039/b402803a>
36. **Xu, H., Liu, F., Cui, Y., Chen, B.L., Qian, G.D.** A Luminescent Nanoscale Metal-Organic Framework for Sensing of Nitroaromatic Explosives *Chemical Communications* 47 (11) 2011: pp. 3153–3155.